Composites: Part A 42 (2011) 1247–1262

Contents lists available at ScienceDirect

Composites: Part A

journal homepage: www.elsevier.com/locate/compositesa

Lightning strike damage resistance and tolerance of scarf-repaired mesh-protected carbon fiber composites

Hirohide Kawakami [1], Paolo Feraboli *

Department of Aeronautics & Astronautics, University of Washington, United States

ARTICLE INFO

Article history:
Received 10 January 2011
Received in revised form 29 April 2011
Accepted 7 May 2011
Available online 14 May 2011

Keywords:
A. Carbon fiber
B. Electrical properties
B. Damage tolerance
Repair

ABSTRACT

Carbon fiber/epoxy composite specimens are manufactured using liquid resin infusion and incorporate a copper wire mesh on the outer layer for lightning strike protection. The specimens are then painted in order to be representative of an aircraft skin. The specimens are subjected to a scarf repair, which removes a portion of the wire mesh and of the carbon fiber substrate. The bonded repair is performed to re-establish the structural and electrical integrity of the laminate. Purpose of the study is to evaluate the effect of repair procedure on the structural performance of the carbon/epoxy specimens following a lightning strike, and in particular it is aimed at comparing the two extreme cases where full electrical conductivity is re-established, and where the electrical conductivity is interrupted. To do so, the copper wire mesh is re-applied during the repair following two scenarios. The first, denoted as "good" repair, involves overlapping part of the repair mesh with the parent mesh surrounding the repair area, while the second, referred to as "poor" repair, involves applying a repair mesh that is shorter than the parent mesh, thereby leaving a gap in the electrical path. The repaired specimens are then subjected to simulated lightning strike at the location of the repair. The damage resistance characteristics of the repaired specimens are compared to the benchmark values of unprotected specimens (i.e. without copper mesh) and protected pristine specimens (i.e. without repair). Residual strength testing using four-point bend flexure is used to assess the damage tolerance behavior of the specimens. Results show that a "good" repair performs as well as the pristine protected specimen, while a "poor" repair performs equally or worse than a fully unprotected specimen.

1. Introduction

Liquid resin infusion technology is being proposed as a low-cost alternative to traditional autoclave/prepreg composite technology. Processes such as VaRTM (Vacuum assisted Resin Transfer Molding) offer lower raw material costs, automated preforming possibility, and the possibility of vacuum-only oven cure, therefore dramatically reducing part-cost and cycle time. JAXA [1,2], Mitsubishi Aircraft [3], Boeing [4] and Lamborghini [5,6] have been investing heavily in Research & Development efforts to manufacture large, complex, integral structures via VaRTM, in order to demonstrate the feasibility of this out-of-autoclave technology.

The introduction of composites in the primary structure of modern aircraft presents special problems with regards to the lighting strike threat. While metallic structures such as traditional aluminum airframes are highly conductive, Carbon Fiber Reinforced Polymers (CFRP) have a much lower electrical conductivity. Although carbon fibers are good conductors, the polymer matrix is an excellent dielectric and therefore reduces the overall conductivity of the composite laminate. When lightning strikes, a large amount of energy is delivered very rapidly, causing the ionized channel to expand with supersonic speed. If the shockwave encounters a hard surface, its kinetic energy is transformed into a pressure rise, which causes fragmentation of the structure. At the same time, resistive heating leads to temperature rise and, in turn, it initiates a breakdown of the resin by pyrolysis. If the gases developing from the burning resin are trapped in a substrate, explosive release may occur with subsequent damage to the structure [7,8]. In order to reduce the threat of lightning strike damage, a lightning strike protection (LSP) is typically utilized. A commonly utilized LSP is a metallic wire mesh, which is placed on the outer surface of the CFRP structure, and acts as a continuously-conductive outer layer to dissipate direct or indirect electromagnetic interference effects. The mesh can be comprised of aluminum, copper or bronze wire, and can either be co-woven with the carbon fiber in a prepreg fabric ply, or bonded separately as the outermost laminate layer [7–9].

* Corresponding author. Address: Automobili Lamborghini Advanced Composite Structures Laboratory, Department of Aeronautics and Astronautics, Box 352400 Guggenheim Hall, University of Washington, Seattle, WA 98195-2400, United States.
E-mail address: feraboli@u.washington.edu (P. Feraboli).
[1] Japan Ministry of Defense, Tokyo, Japan.

1359-835X/$ - see front matter © 2011 Elsevier Ltd. All rights reserved.
doi:10.1016/j.compositesa.2011.05.007

Lightning strike damage poses both a safety and economic challenge for aircraft manufacturers and operators [9–11], however limited work has been published to assess the structural performance of CFRP specimens following lightning strike damage [12]. In previous studies [13,14], the authors inflicted simulated lightning strike damage at different current levels on carbon/epoxy specimens in order to characterize their damage resistance and tolerance response. Test articles included both unnotched and filled-hole specimens, and were unpainted and unprotected. After damage was inflicted, the CFRP specimens were tested for residual strength in tension, compression, or compression after impact (CAI). An attempt was made to establish a comparison between mechanical impact damage, such as traditional foreign object damage (FOD) associated with low-velocity, drop-weight impact and lightning strike damage.

FOD is a known threat to composite structures, and the damage-tolerant design philosophy of the building block approach is intrinsically tied to the concept of FOD [15–18]. As an example, margin of safety calculations for static strength determination are directly tied to the definition of acceptable and detectable damage, which is in turn tied to inspection and repair strategy. Typical sources of FOD can include mishandling during manufacturing, tool drop during service, hail strike, bird strike, as well as lightning strike. The maintenance strategy has to define a threshold of detectability and a method of inspection, which is usually visual. If the damage is too small to be detected, it shall be neglected and its presence shall not reduce the ultimate strength of the structure. On the other hand, if the damage is sufficiently large, it should be discovered and repaired, while temporarily accepting a reduction in strength [15,17]. Once repaired, the structure shall return to the same strength, and be subject to the same requirements as the original structure before damage and repair.

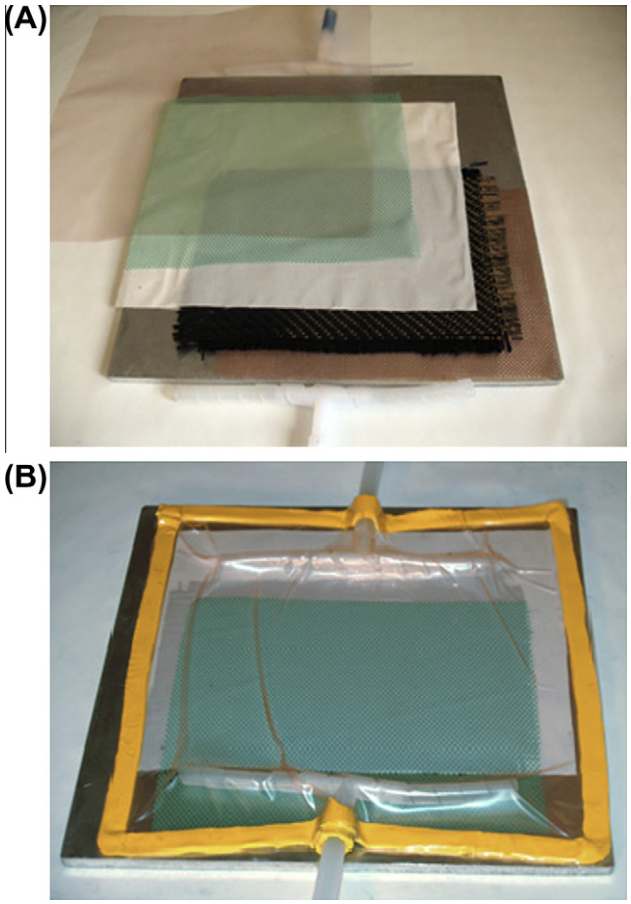

Fig. 1. (A and B) Liquid resin infusion of the panels: (A) before infusion and (B) after infusion. (For interpretation of the references to color in this figure legend, the reader is referred to the web version of this article.)

Bonded scarf repairs have been widely used to repair composite structures and, with the appropriate surface preparation and a validated process, they can offer the greatest structural efficiency of all repairs [18–20]. While extensive research has been focused to determine how bonded scarf repair can be used to re-establish the structural integrity of a CFRP structure, the new challenge imposed by the threat of lightning strike damage imposes researchers to focus on the effect of bonded scarf repairs on the electrical integrity of a CFRP structure. Since the scarf operation removes the copper wire mesh LSP, as well as the underlying damaged portion of the laminate, the electrical flow path is interrupted unless an additional repair mesh is placed on the outer skin. However, questions arise whether it is necessary that the repair mesh overlap the parent mesh in order to fully re-establish the conductive path, or if it is sufficient for the mesh to be in proximity of the parent mesh, thereby allowing for gaps to exist between the repair and parent meshes. From a procedural standpoint it would be easier not to overlap the meshes, since doing so would create a surface irregularity, which in turn would affect aerodynamic drag during flight, or would otherwise require extensive sanding and finishing or painting operations. The experimental evidence presented here aims at understanding the effect of having a "good" or "poor" repair from an electrical conductivity standpoint, by subjecting CFRP laminates to lightning strike damage and assessing their damage resistance and tolerance characteristics. Ultimately, the research aims at providing a guideline for best practice for scarf repairs of exposed (on the outside of the aircraft) CFRP structures, featuring a copper wire mesh LSP.

2. Experimental procedure

2.1. Specimen manufacturing and preparation

Dry fabric of T300 carbon fiber with 3 K tow, 2 × 2 twill weave fiber architecture are infused with an untoughened, low-viscosity, 284 F (140 °C) cure epoxy resin, designed for VaRTM processing. The dry fabric used is Hexcel Prime Tex™ ZB Fabric style 284, an aerial weight of which is 5.78 oz/yd^2 (196 g/m^2). The resin and hardener of the epoxy resin are Huntsman Resin XB 3518 BD and Aradur® 22962, respectively. Initial mix viscosity of the resin is

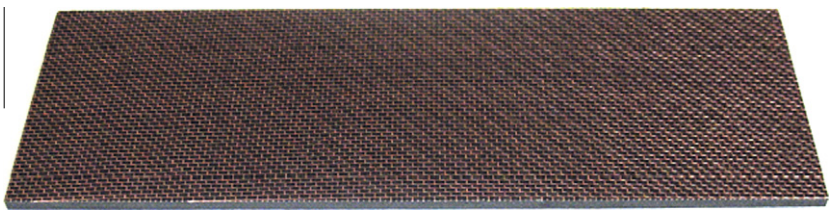

Fig. 2. Typical specimen with LSP (wire copper mesh) after infusion and curing. (For interpretation of the references to color in this figure legend, the reader is referred to the web version of this article.)

30–60 mPa s at 140 F (60 °C). For the unprotected specimens, rectangular flat specimens 14 in. × 10 in. (356 mm × 254 mm) are fabricated using 20 layers of cloth in the (0/90) direction for a nominal thickness of 0.160 in. (4.1 mm). Consumable materials used during the infusion include the peel ply (AIRTECH Release Ply B), the reticulated flow media (AIRTECH Greenflow 75) used to facilitate the infusion process, the line ports for resin injection, the line port for the air and vacuum suction, the nylon vacuum bag (AIRTECH Ipplon DP1000), and sticky tape sealant, Fig. 1A and B. For the protected specimens, a copper wire mesh on the outer surface of the laminate provides the LSP (lightning strike protection). The mesh size is 16 × 16 per lineal inch (or every 25.4 mm), thickness is 0.020 in. (0.5588 mm), and wire diameter is 0.011 in. (0.28 mm). The wire's characteristics are typical of standard woven mesh for

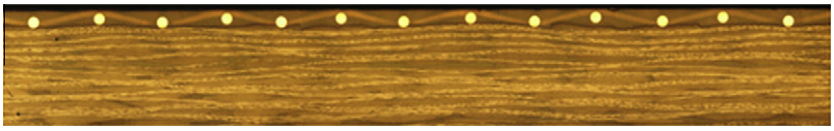

Fig. 3. Typical cross section of laminate with wire copper mesh, showing negligible amount of voids. (For interpretation of the references to color in this figure legend, the reader is referred to the web version of this article.)

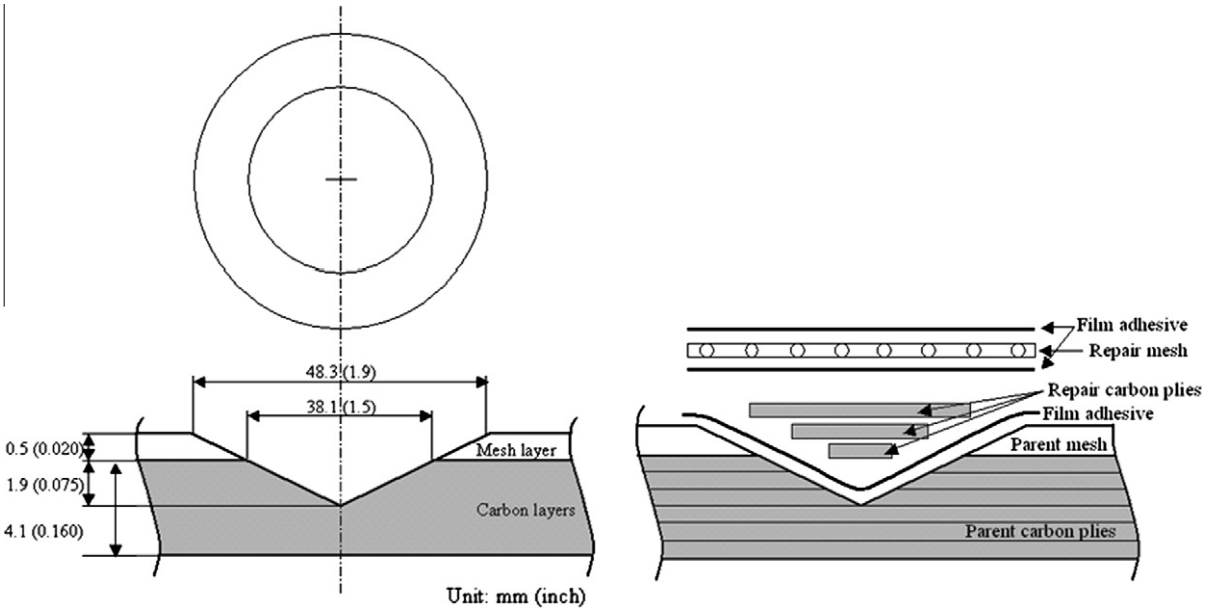

Fig. 4. Schematic of scarf repair patch and materials.

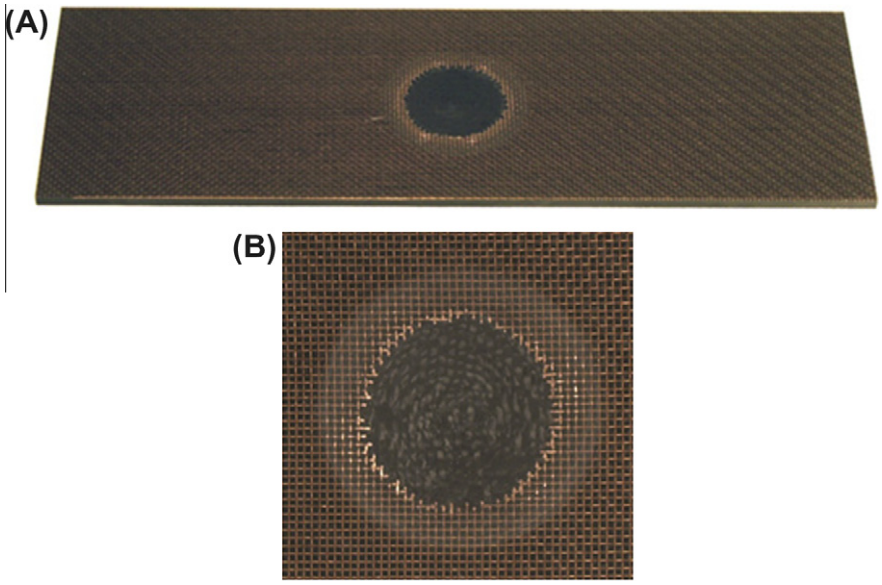

Fig. 5. (A and B) Specimen with copper mesh: after scarfing (A) and detail of the scarf area (B). (For interpretation of the references to color in this figure legend, the reader is referred to the web version of this article.)

Fig. 6. Kit of precut repair materials as they are placed into the scarf area (from the bottom outward, from left to right): film adhesive, eight patch plies of different dimensions, film adhesive, repair mesh, film adhesive. (For interpretation of the references to color in this figure legend, the reader is referred to the web version of this article.)

electromagnetic shielding. The supplier of the copper wire is TWP Inc. The copper mesh is placed on the tool-side surface as an additional ply for the laminate prior being infused. The cured laminate thickness of the protected specimens becomes 0.180 in. (4.6 mm). For both protected and unprotected specimens, the following infusion process and cure cycle are used: (1) preparation of the mold, dry carbon fiber fabrics and other materials and then bagging, (2) Debulking the bag under applied full vacuum (28 in Hg (94.8 kPa)) at 140 F (60 °C) for 30 min, (3) resin preparation and degassing at 28 in Hg (94.8 kPa) for 10 min, (4) resin impregnation to the vacuum bag at 140 F (60 °C), (5) Curing the specimen in a oven at 212 F (100 °C) for 1 h and then further curing at 284 F (140 °C) for 2 h, (6) cooling the bagged specimen down to room temperature then debagging. After curing, test specimens are machined and trimmed to the final dimensions of 12 in. × 4 in. (305 mm × 102 mm). Based on prior experience [13,14], these dimensions are chosen because they are sufficiently large to contain the lightning strike damage well within the boundaries and, at the same time, are suited for the residual strength testing by four point bending. A typical protected specimen after trimming is shown in Fig. 2. Accurate selection of process and equipment enables the manufacturing of high quality laminates with negligible voids, Fig. 3. A total of 40 specimens are manufactured using this process.

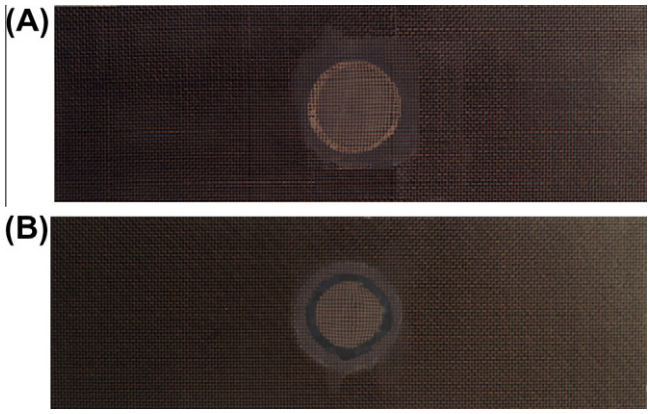

Fig. 7. (A and B) Two types of repair specimens: "good" repair (A) and "poor" repair (B) showing overlap and gap respectively between the repair mesh and parent mesh. (For interpretation of the references to color in this figure legend, the reader is referred to the web version of this article.)

After manufacturing, 18 of the 40 specimens are prepared for structural repair, in the same way that they would be handled in service if damage were to be discovered during routine inspection. It should be emphasized that there is no actual damage to the laminates, but the repairs are performed "as if" they were damaged. The repair procedure is a bonded scarf repair, which requires removal of a portion of material at and around the location of the damage, Fig. 4. It is assumed that the damage is contained within the upper portion of the laminate, so the depth of the machined (scarf) area is 0.075 in. (1.9 mm). The scarf ratio selected is 20:1, which is the typical value suggested by the MIL-HDBK-17 [18]. The outermost diameter of the scarf area is 1.5 in. (38.1 mm) for the unprotected specimen, and 1.9 in. (48.3 mm) for the specimen with copper mesh. The schematic of the repair and the materials used are shown in Fig. 4. The scarf is machined by grinding to a rough shape with a hand rotary tool, trimming with 100 grit sand paper bonded to an aluminum circular cone designed for this specific scarf dimension, finishing with 320 grit sandpaper, cleaning and drying the specimen. A typical specimen with copper mesh following the scarfing procedure and prior to application of the patch plies is shown in Fig. 5A and B. For the patch repair material, TORAYCA T700S/2510 carbon fiber/epoxy prepreg and 3M AF126-2 structural film adhesive are used. The patch material plies, film adhesive, and copper mesh outer layer are cut to the required dimensions, Fig. 6. A sheet of film adhesive is first placed on the bottom of the scarf hole in order to fill the gap between the hole and the stack of plies. Starting from the smallest, the individual prepreg patches are positioned and compacted. Another layer of film adhesive is applied before positioning of the repair copper mesh, and finally a last layer of film adhesive is used to further ensure that the surface is not resin-starved. Curing of the patch is performed using a Heatcon commercial dual zone hot-bonder setup, and a heat stretch blanket. The patch is cured for 120 min at 270 F (132 °C) under vacuum pressure.

The specimens referred to as "good" repair feature a full overlap of the repair mesh over the parent mesh material (+0.125 in. or +3.18 mm around the circumference of the patch). This length is selected because it ensures that the electrical conductivity in the mesh is fully re-established between the parent and the patch

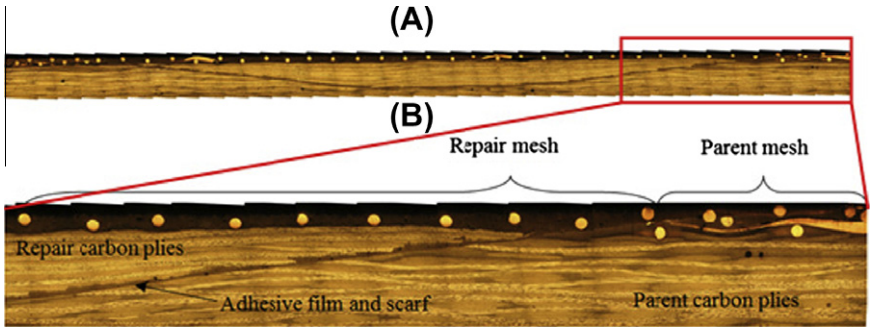

Fig. 8. Micrographic cross-section of scarf repair specimen with mesh overlap (A) and detail of scarf area (B). (For interpretation of the references to color in this figure legend, the reader is referred to the web version of this article.)

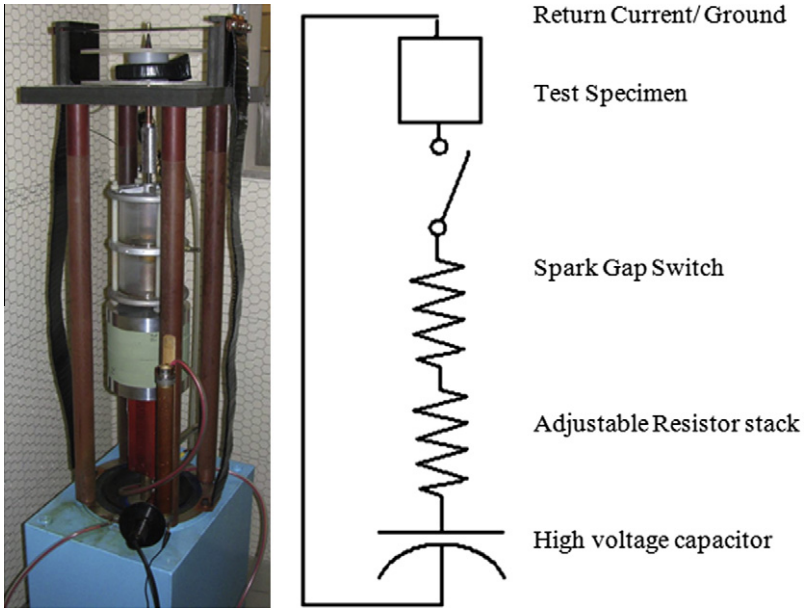

Fig. 9. Picture and schematics of the lightning strike generator. (For interpretation of the references to color in this figure legend, the reader is referred to the web version of this article.)

material, Fig. 7A. The specimens referred to as "poor" repair feature a repair mesh which stops short of the parent mesh material (the gap is −0.125 in. or −3.18 mm around the circumference of the patch). This length is selected because it ensures that the electrical conductivity in the mesh is not fully re-established between the parent and the patch material, Fig. 7B.

A typical cross-section of the repaired specimen with copper mesh, Fig. 8A, shows the scarf region, with the tapered patch of repair plies isolated from the parent laminate by the layer of film adhesive. A close-up of the scarf region, Fig. 8B, also shows the overlap of the repair mesh with the parent mesh, which is what is expected for a so-called "good" repair specimen. Finally, a portion of the specimens is coated by aircraft-grade acrylic paint, which is a perfect dielectric in terms of electrical conductivity.

2.2. Damage infliction and evaluation

The lightning strike generator developed at the University of Washington is employed for this research. A schematic of the generator is shown in Fig. 9, and details can be found in [13,14]. The capacitor is capable of supplying 44 kV and 52 μF, and the

Table 1
Summary of test families and conditions (N indicates NO, Y indicates YES).

Family	Paint	Mesh protection	Patch repair	Repair mesh	Subject to strike	Subject to residual strength testing
N0	N	N	N	N	N	Y
MP0	Y	Y	N	N	N	Y
R0	Y	Y	Y	Overlap or gap	N	Y
N80	N	N	N	N	Y	Y
P80	Y	N	N	N	Y	Y
M80	N	Y	N	N	Y	Y
MP80	Y	Y	N	N	Y	Y
GR80	Y	Y	Y	Overlap	Y	Y
PR80	Y	Y	Y	Gap	Y	Y

Fig. 10. Details of the test specimen area of the lightning strike generator. (For interpretation of the references to color in this figure legend, the reader is referred to the web version of this article.)

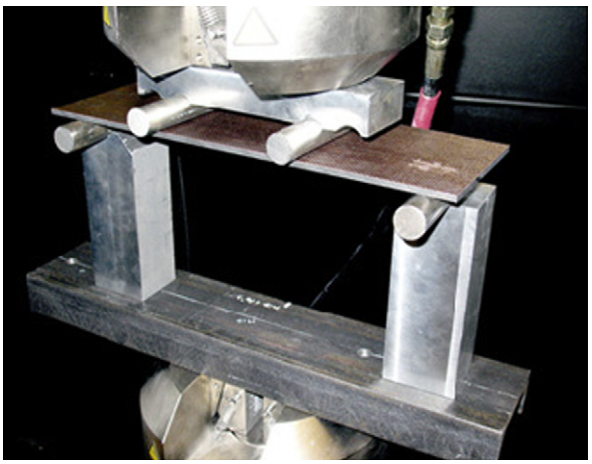

Fig. 11. Four point bend flexure test setup for residual strength testing. (For interpretation of the references to color in this figure legend, the reader is referred to the web version of this article.)

adjustable resistor stack is used to modulate the waveform. The lightning generator is used to generate a current pulse similar to waveform D, specified in SAE ARP 5412 [21], with peak amplitude of 80 kA. Waveform D has peak current amplitude of 100 kA, represents a typical re-strike, and is used to certify the vast majority of the airframe, unlike waveform A that is used only for primary attachment points [21] at the wing tips, nose or empennage. A spark gap switch is used to trigger the strike, Fig. 9. The test specimen is installed in the top of the generator, right above the conical electrode (striker) and it is supported at the two short ends between two return copper electrodes, as shown in Fig. 10. The specimen is placed with the copper mesh and or repair surface facing the striker, at a distance of 0.75 in. (19.1 mm). After introducing the lightning strike damage, a non-destructive inspection is performed via pulse-echo ultrasound using a C-scan system with a 2.25 MHz sensor. The projected damage area of all the specimens is then measured using image analysis software. One specimen from each test configuration is then selected for destructive inspection, which is performed by cross-sectioning and optical microscopy. Two micrographic coupons are extracted from a single specimen at the attachment point of the lightning strike, one parallel to the 0° fibers, and one transverse to them. The 0° fibers run in the direction of the electrodes, located at the end of the specimen. To avoid losing the information on the strike, a two-stage mount with laser dye is employed [13,14]. At the strike location, carbon fiber and epoxy are melted or vaporized, thereby making

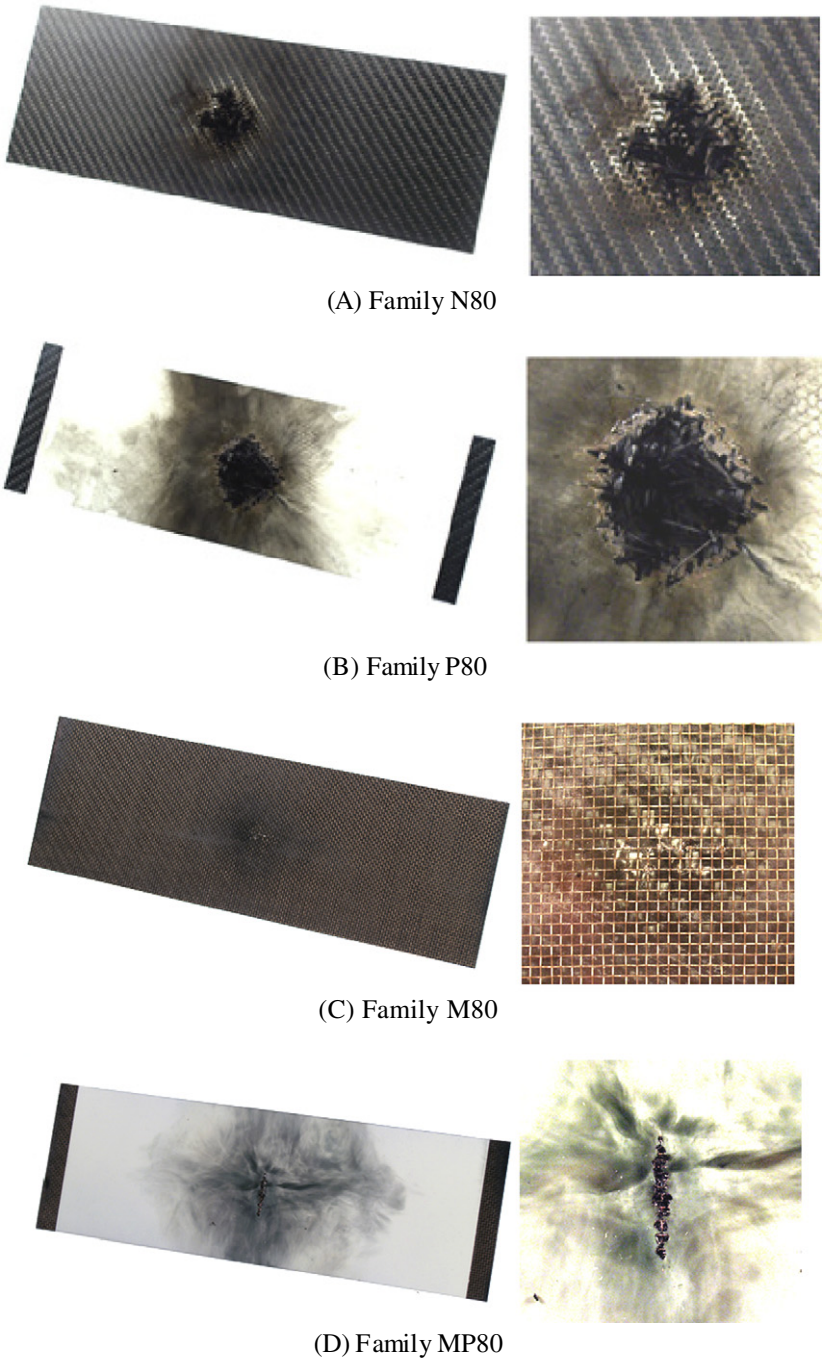

Fig. 12. (A and D) Visual and close-up view of LSP specimen after strike, unpainted and unprotected (N80), painted and unprotected (NP80), unpainted and protected (M80), and painted and protected (MP80). (For interpretation of the references to color in this figure legend, the reader is referred to the web version of this article.)

the entire area very delicate and fragile. Laser dye epoxy is used to distinguish between the composite specimen's epoxy and the mounting epoxy.

A summary of the nine specimen families tested is reported in Table 1, where N indicates natural condition, M indicates the presence of the copper mesh protection, P indicates painted surface, GR indicates a "good" repair, PR a "poor" repair, and the numbers 0 and 80 indicate if the laminate has been subjected to lightning strike damage at 80 kA. These include three benchmark families, which are not subjected to lightning strike damage (N0, MP0, and R0), and are used to established the pristine flexural strength for the other families. These three families indicate respectively: unprotected, unpainted, non-repaired specimen (N0), mesh-protected, painted, non-repaired specimen (MP0), and mesh-protected, painted, repaired specimen (R0). In this case whether the repair is "good" or "poor" is not relevant since these benchmark families are not subjected to lightning strike, and structurally there is no difference between a poor and good repair. Purpose of comparing these three families is to establish the effect of the mesh and paint on flexural strength, and to assess the quality of the repair and compare it against the pristine specimens. Families N80 and P80 indicate unprotected, non-repair specimens that are both subjected to lightning strike damage, but without and with the paint layer respectively. Purpose of the comparison is to evaluate the effect of the dielectric paint layer on damage size and residual strength. Similarly, families M80 and MP80 represent specimens with copper mesh protection, without and with paint respectively, and subjected to lightning strike damage. These two families provide information with regards to the effectiveness of the copper mesh in alleviating the damage from the lightning strike. Lastly, families GR80 and PR80 represent mesh protected, painted and repaired specimens subjected to lightning strike damage, in presence or absence respectively of fully-re-established electrical conductivity between repair and parent material.

2.3. Residual strength assessment

Damage tolerance testing is conducted in a universal test frame at quasi-static loading conditions. A fixture for four-point bend flexure (4PBF) is used for residual strength testing of the specimens, Fig. 11. Although other tests could be used for damage tolerance assessment, such as compression after impact (CAI) [14], flexure testing is typically used for composite repair testing and for sandwich panels [20] because it induces a pure flexural state

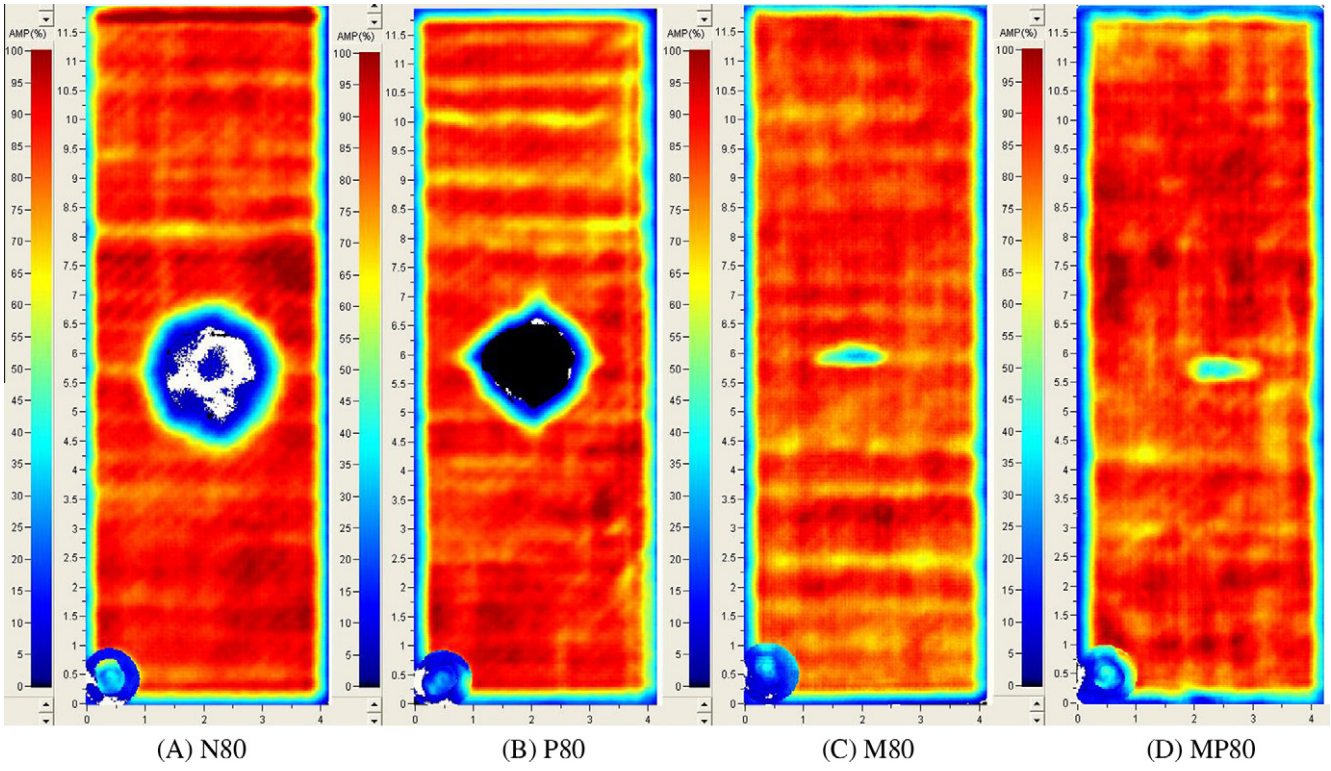

Fig. 13. (A and D) Ultrasonic C-scan images of specimens N80, P80, M80, and MP80. (For interpretation of the references to color in this figure legend, the reader is referred to the web version of this article.)

Table 2
Summary of lightning strike damage tests and results.

Family	Repeats	Description of damage	Avg. damage area (in.^{2}) (mm^2)	CoV damage area (%)
N80	4	Fiber fracture, outer plies bulging, matrix vaporization	3.922 (2530)	8
P80	4	Fiber fracture, outer plies bulging, matrix vaporization	2.865 (1848)	11
M80	4	Outer paint and matrix burning, copper mesh minor pitting	0.153 (99)	52
MP80	4	Outer paint and matrix burning, copper mesh minor pitting	0.277 (179)	37
GR80	6	Outer paint and matrix burning, copper mesh minor pitting	0.157 (101)	53
PR80 Type I	2	Outer paint and matrix burning, copper mesh minor pitting	0.219 (141)	69
PR80 Type II	4	Circular annulus of burn marks and fracture around patch	3.069 (1980)	5
PR80 Type III	3	Entire patch is separated from repair, with evidence of burn marks and fracturing	5.572 (3595)	29

of stress at the midspan of the specimen. However, upon large specimen deflection, a combined flexural and out-of-plane normal (peel) stress state is generated, which tends to separate the patch repair from the parent laminate. 4PBF is therefore a better indicator of good bond quality for a repair than the CAI test.

The specimen is placed on the support rollers with the mesh and repair side facing up, on the compressive side. The inner and outer spans of the loading are 4.0 in. (102 mm) and 10.0 in. (254 mm), respectively [22]. The outer span to thickness ratio is 56:1 for a specimen with mesh and 63:1 for a specimen without mesh. The large span to thickness ratio is employed in order to reduce the effects of shear and to increase bending deformation and, hence, peel stresses. The inner span is sufficiently large to extend over the entire patch. The loading and support noses are steel cylinders of 0.75 in. (19.1 mm) diameter. To avoid premature damage by the stress concentration in the proximity of the supports, the specimen needs to be loaded with large-radius loading rollers. A summary of the specimen families is reported in Table 1.

3. Results

3.1. Damage resistance: damage analysis and inspection

For the unprotected specimens, both unpainted N80 and painted P80, a large circular damage was centered at the lightning

Fig. 14. Visual and close-up view of GR80. (For interpretation of the references to color in this figure legend, the reader is referred to the web version of this article.)

(A) Family PR80, Type I damage

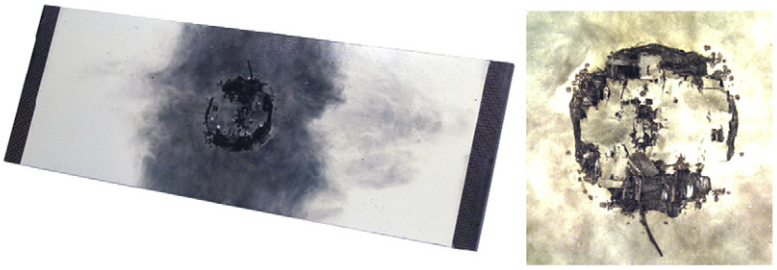

(B) Family PR80, Type II damage

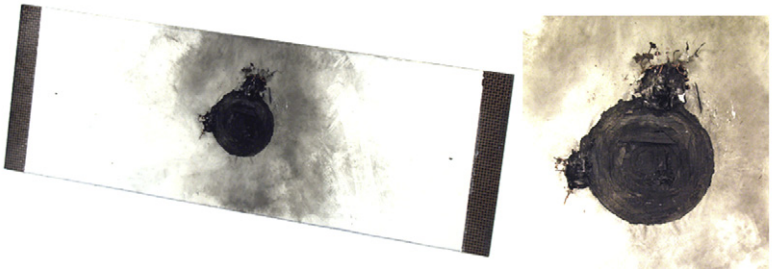

(C) Family PR80, Type III damage

Fig. 15. (A and C) Visual and close-up view of PR80 Type I damage (A), Type II damage (B), Type III damage (C). (For interpretation of the references to color in this figure legend, the reader is referred to the web version of this article.)

attachment point as shown in Fig. 12A and B and in the ultrasonic scans of Fig. 13A and B. Fractured fibers were clearly visible at the center of the strike location, while evaporation of the surrounding matrix created visible bulging. Damage was concentrated toward the surface of the specimen and confined to the outer plies. Individual surface burns to the paint layer could be observed over a broader area, and were due to the attachment points of the secondary lightning leaders that branched out from main lightning channel. A summary of the results is reported in Table 2, and shows that the average projected damage area for the painted specimens was smaller than the unpainted specimens. Specimens with copper mesh protection, both unpainted M80 and painted MP80, suffered only minor surface damage, which consisted of surface pitting, matrix burning and partial copper wire melting. Damage in the composite ran along the copper wire mesh, and tends to be more severe and deeper at the intersection point of two wires. Two specimens are shown in Fig. 12C and D, while ultrasonic images are shown in Fig. 13C and D. The damage shape was always elongated in the direction perpendicular to the current flow, although the location varied from specimen to specimen. With copper mesh protection, the projected damage area was less than an order of magnitude smaller than in the case of the unprotected specimens, and the depth as well as morphology of damage was significantly different.

For specimens that have undergone scarf repair, the state of damage was dramatically different depending on the quality of the repair. For specimens with good repair GR80, where the repair mesh overlaps the parent mesh, the results were virtually identical to the unrepaired, protected specimens (M80 and MP80), Fig. 14. Visible damage was small and had the same elongated appearance. For specimens with poor repair PR80, three different possible states of damage could be encountered, Fig. 15A–C. In Type I damage, the lightning attached away from the center of the specimen and inflicted damage on the parent material outside the patch repair, Fig. 15A. In Type II damage, the damage ran along the entire circumference of the patch, with clearly visible fiber and matrix burning and vaporization, giving the appearance of a circular annulus of damaged material, Fig. 15B. In Type III damage, the entire patch was detached from the specimens, leaving the scarf area completely empty, with other evidence of burning around the circumference, Fig. 15C. For both Type II and Type III damage, the lightning attachment point was the center of the patch, with secondary leaders attaching to the edge of the repair patch. Statistically speaking, 7 of the 9 specimens tested with poor repair happened to be struck in the center of the patch (Type II and III damage), while only 2 were struck outside the patch (Type I).

For Type I damage, the state of damage was nearly identical to the pristine (M80 and MP80) and good repair specimens (GR80),

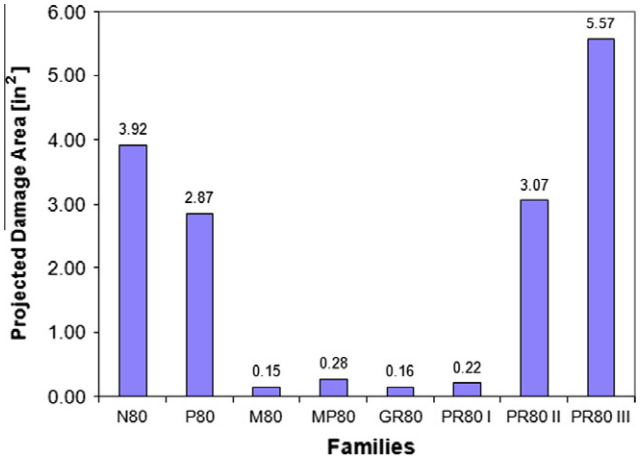

Fig. 17. Plot of the average projected damage area for all families tested. (For interpretation of the references to color in this figure legend, the reader is referred to the web version of this article.)

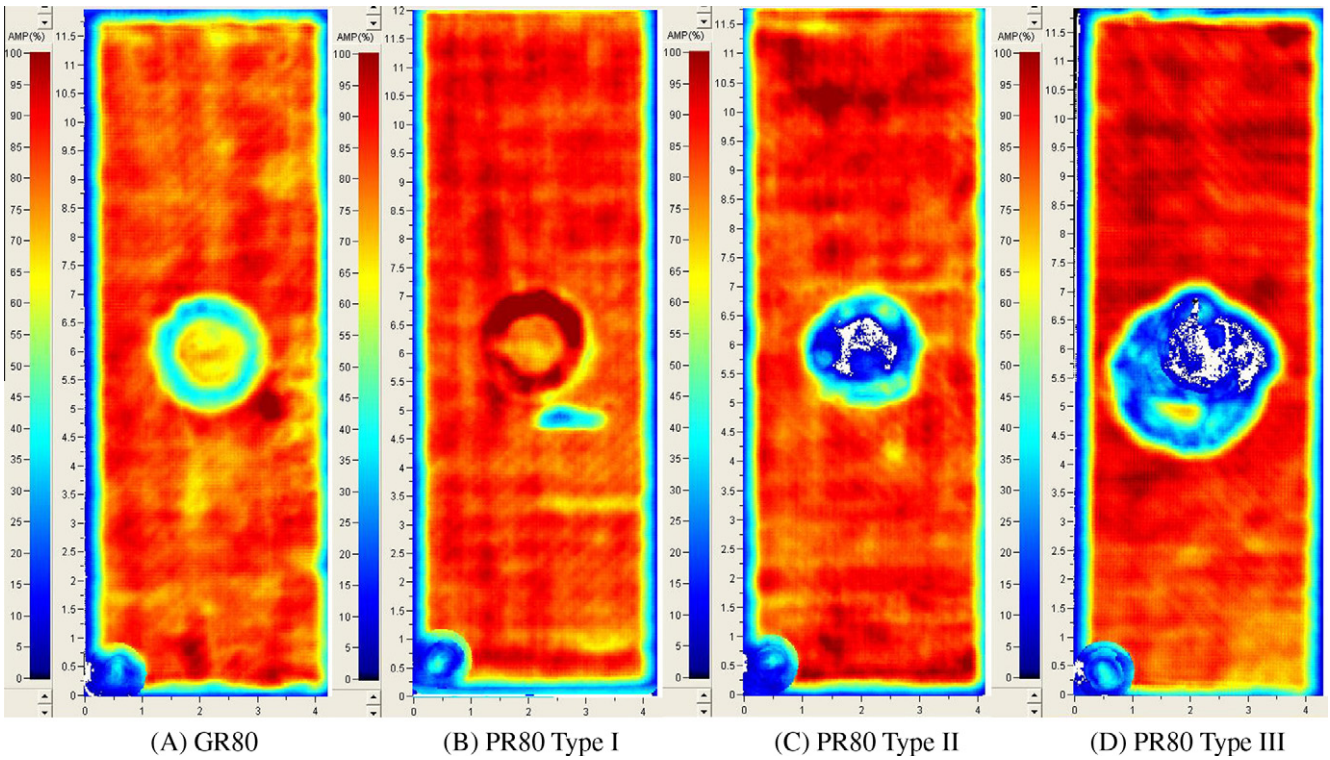

Fig. 16. (A and D) Ultrasonic C-scan images of specimens GR80 (A), PR80 Type I (B), PR80 Type II (C), and PR80 Type III (D). (For interpretation of the references to color in this figure legend, the reader is referred to the web version of this article.)

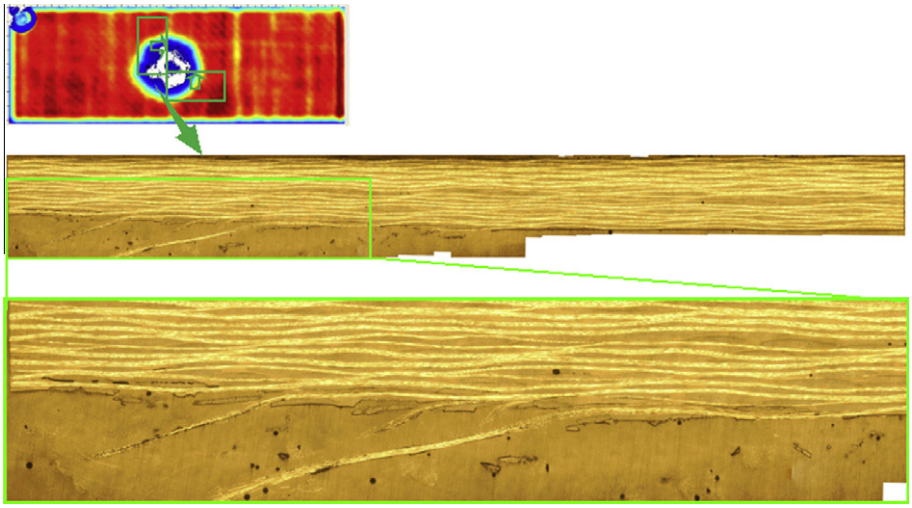

Fig. 18. Microscopy of specimen N80. (For interpretation of the references to color in this figure legend, the reader is referred to the web version of this article.)

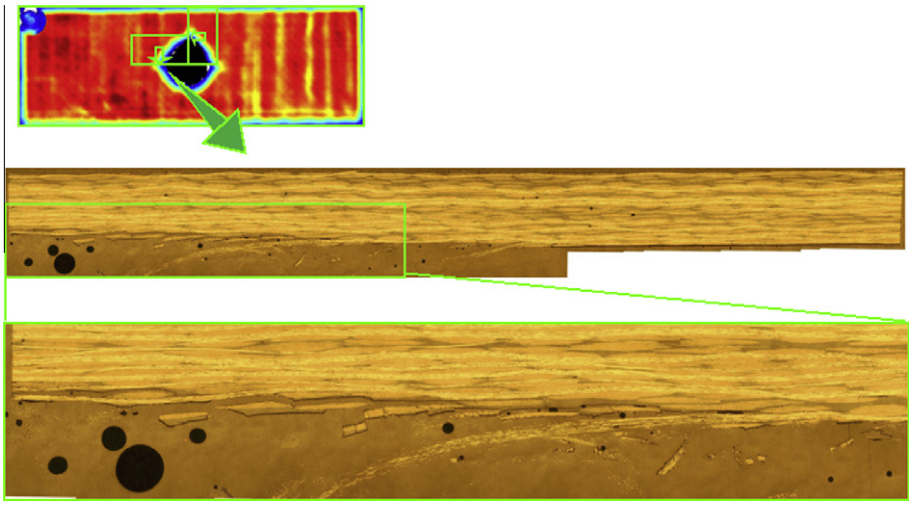

Fig. 19. Microscopy of specimen P80. (For interpretation of the references to color in this figure legend, the reader is referred to the web version of this article.)

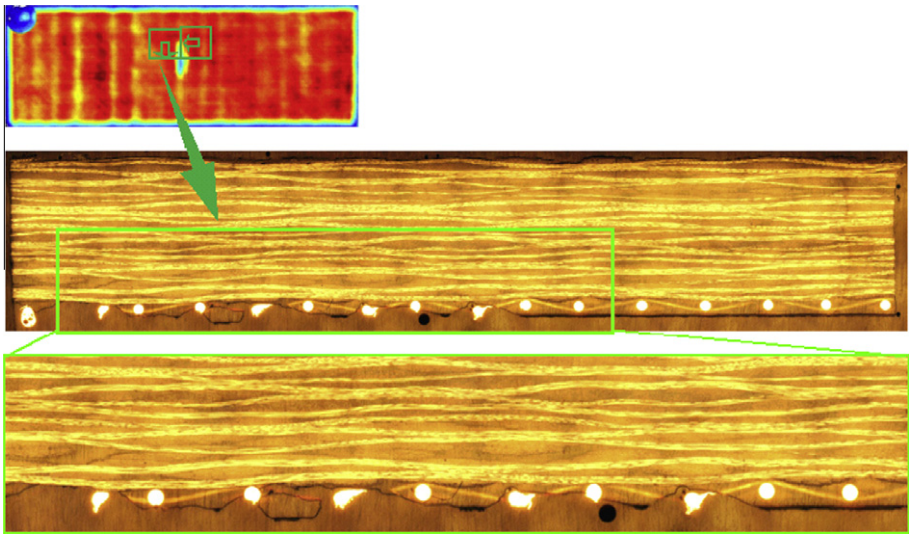

Fig. 20. Microscopy of specimen MP80. (For interpretation of the references to color in this figure legend, the reader is referred to the web version of this article.)

since the lightning current path was not affected by the presence of the electrical discontinuity at the location of the repair. For Type II and III damage, the state of damage was devastating, regardless of whether the patch flied off from the parent laminate. Ultrasonic scans for the GR80 specimen and three types of PR80 specimens are reported in Fig. 16A–D, while a summary of the results is reported in Table 2. For PR80 Type I damage, the average projected damage area was similar to the families M80, MP80 and GR80; for PR80 Type II damage, the damage area was similar to the families N80 and P80; for PR80 Type III damage, the damage area was even larger than for the unprotected specimens. A plot of the average projected damage area for all families tested is reported in Fig. 17.

Two microscopy specimens were extracted from one specimen for each of the various configurations tested. Specimens N80 and P80 showed that lightning damage affected the outermost plies, Figs. 18 and 19, while the majority of the laminate thickness appeared unaffected. There was no major difference in damage between the 0 and 90° directions. Carbon fiber breakage and fiber outward splaying were seen through the two-stage mounting process utilized. Cracks and small delaminations emanated from the center of the specimen and propagated out and through the specimen. For the specimens with copper mesh, both pristine MP80 and good repairs GR80, damage was confined to the

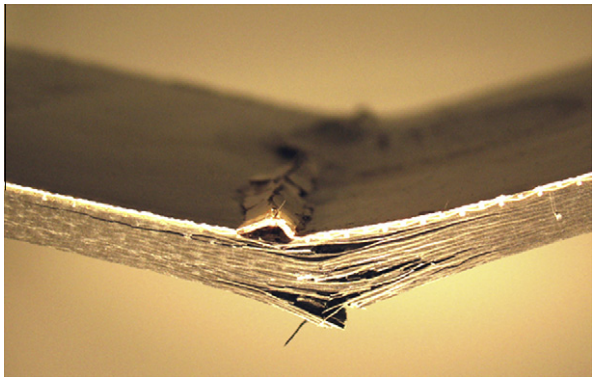

Fig. 23. Typical flexural failure, with tensile fiber breakage on the lower side and compressive kinking of fibers and copper mesh on upper side. (For interpretation of the references to color in this figure legend, the reader is referred to the web version of this article.)

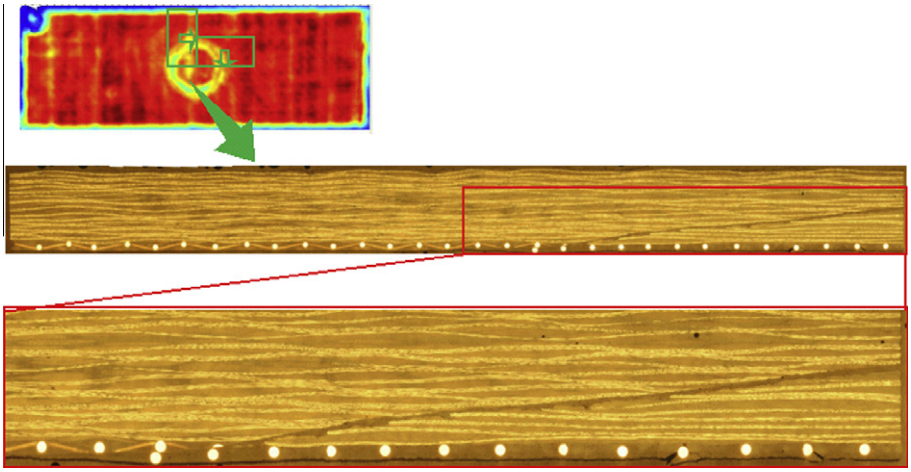

Fig. 21. Microscopy of specimen GR80. (For interpretation of the references to color in this figure legend, the reader is referred to the web version of this article.)

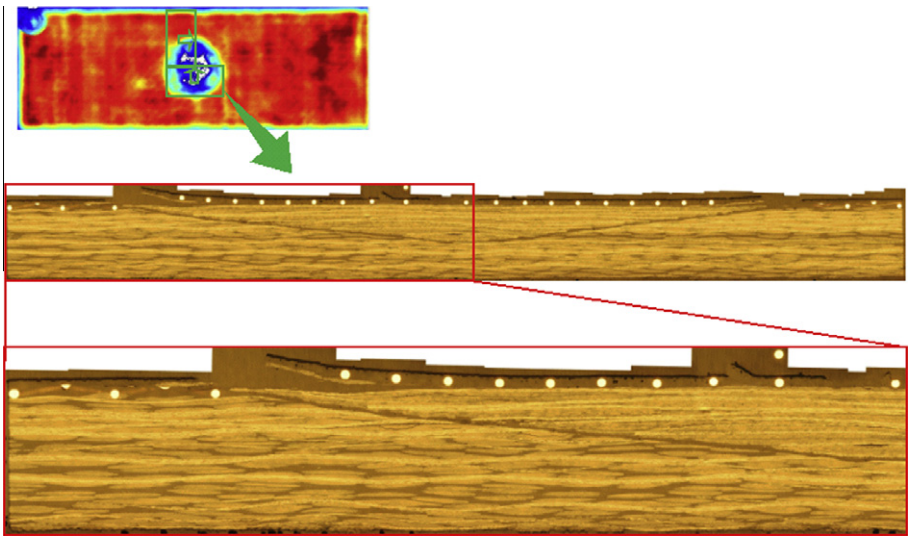

Fig. 22. Microscopy of specimen PR80, Type II damage. (For interpretation of the references to color in this figure legend, the reader is referred to the web version of this article.)

protective copper mesh and the outermost carbon fiber ply, as shown in Figs. 20 and 21. Small cracks and delaminations were visible over the copper mesh and at the interface between the mesh and the outer ply. Some resin showed evidence of burning, and small areas of copper mesh showed pitting and melting.

The damage state of PR80 Type II specimens, Fig. 22, was devastating. Damage was dispersed throughout the entire repair patch, and was not contained to even the patch. Within the patch, it reached halfway past the midplane of the thickness, which was deeper than in the case of unprotected specimens. Some cracks penetrated the layer of film adhesive between the patch and parent material, and propagated through the parent material. Severe damage could be seen at the center and edges of the repair patch, i.e. peeling of the copper mesh layer, and carbon fiber breakage and splaying, and vaporization of the epoxy matrix. These fracture behaviors were similar to the damage of the unprotected specimens at the lightning attachment point. PR80 Type I and Type III damage were not significant for microscopic evaluation.

In summary, according to visual, ultrasonic, and microscopic inspection, the state of damage in the families tested can be classified in the three categories: (A) minor damage on the copper mesh layer and the adjacent carbon layer (families M80, MP80, GR80 and PR80 Type I); (B) severe damage to the outer plies (families N80, P80 and PR80 Type II); and (C) repair patch flies off and damage spreads out over the parent material (family PR80 Type III).

Table 3
Summary of residual flexural strength test results (N indicates NO, Y indicates YES).

Family	Repeats	Lightning damage	Avg. residual strength [ksi] (MPa)	CoV residual strength (%)	Normalized residual strength/ pristine strength
N0	3	N	105.6 (728)	2.3	1.00
N80	4	Y	91.9 (633)	3.9	0.87
P80	4	Y	85.9 (592)	4.2	0.81
MP0	3	N	106.6 (735)	0.6	1.01
M80	4	Y	106.1 (731)	7.4	1.00
MP80	4	Y	106.4 (733)	2.1	1.01
R0	3	N	103.8 (716)	2.1	0.98
GR80	6	Y	106.5 (734)	6.2	1.01
PR80 Type I	2	Y	101.2 (698)	5.7	0.96
PR80 Type II	4	Y	90.4 (623)	3.5	0.86
PR80 Type III	3	Y	64.1 (442)	16.0	0.61

3.2. Damage tolerance: residual strength

All specimens failed simultaneously by compressive fiber kinking on the upper side, and tensile fiber fracture on the lower side,

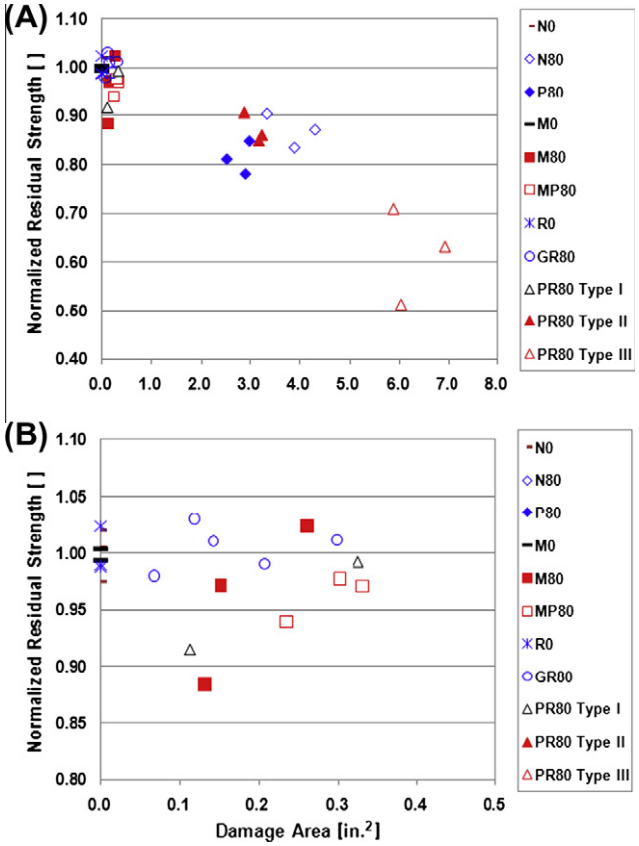

Fig. 25. (A and B) Normalized residual strength vs. damage area, showing the grouping into three major damage scenarios for all families (A), and close-up of the area around the 100% strength (B). (For interpretation of the references to color in this figure legend, the reader is referred to the web version of this article.)

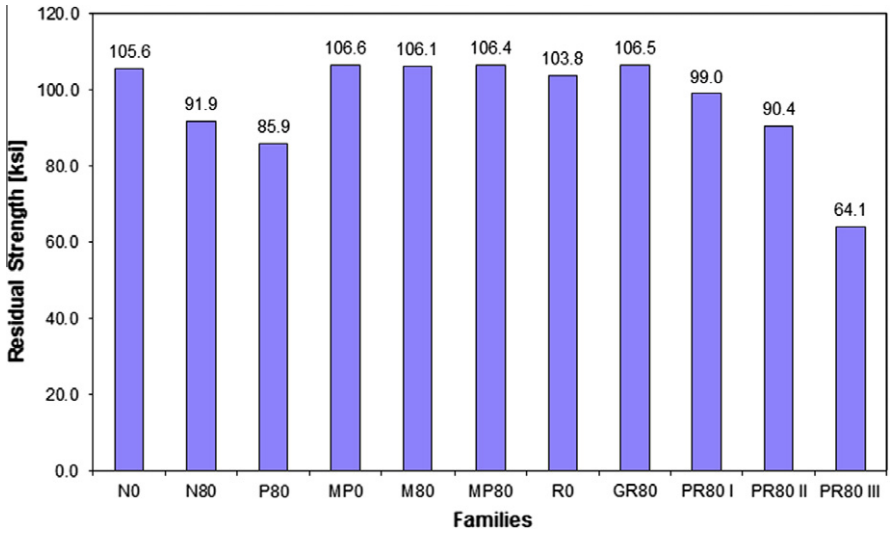

Fig. 24. Residual flexural strength properties for each of the families tested. (For interpretation of the references to color in this figure legend, the reader is referred to the web version of this article.)

Fig. 23. For specimens with copper mesh, the ductile copper bent extensively out of the plane after locally buckling, and separated from the composite substrate. A summary of the residual strength results for all families is reported in Table 3 and plotted in Fig. 24. For specimens with copper mesh, the flexural strength is calculated using only the carbon fiber laminate thickness, thereby assuming that the contribution of the copper mesh is negligible. It can be seen that the lightning strike damage reduced the flexural strength significantly in the absence of copper mesh protection, and more so for specimens with paint (P80) than without (N80), as compared to the baseline (N0). Results also confirm that the copper mesh had no influence on the pristine strength of the laminate (MP0), as compared to the baseline unprotected strength (N0). Specimens with repair (R0) performed identically to the pristine ones (N0 and MP0), therefore confirming that the repair procedure was of high quality and structural integrity was re-established. Specimens with mesh protection were substantially unaffected in terms of residual strength by the presence of the lightning damage (M80 and MP80) and, similarly, "good" repair specimens (GR80) and "poor" repair specimens displaying Type I damage (PR80 Type I). On the other hand "poor" repair specimens with Type II damage morphology (PR80 Type II) exhibited a similar strength reduction to the unprotected specimens (N80 and P80), while PR80 Type III specimens exhibited an even greater reduction in residual flexural strength due to the absence of the repair patch, and therefore a reduced load-bearing capability.

Normalizing all strength values by the strength of the pristine, unpainted, unprotected, unrepaired strength (N0), it is possible to obtain the plot in Fig. 25A with dimensionless values. From this plot, it can be seen that all strength values can be grouped into three broad categories, corresponding to the categories of damage A–C discussed in the previous section. Category A is grouped around the pristine value 1.00 (no strength reduction). A close-up of this region is reported in Fig. 25B, and includes families N0, MP0, M80, MP80, R0, GR80 and PR80 Type I. Category B, which is clustered around the normalized value of 0.85 (15% reduction), includes families N80, P80 and PR80 Type II. Finally, Category C, with an average value of 0.60 (40% reduction), includes solely family PR80 Type III. There was significant variation amongst the data, particularly in terms of damage area (Table 2), with Coefficient of Variation (CoV) as high as 60% in some cases, while in terms of residual strength the CoV was much lower (Table 3). This type of variation is typical of lightning strike damage tolerance investigations [14] due to the variety of factors that can affect the resulting damage state.

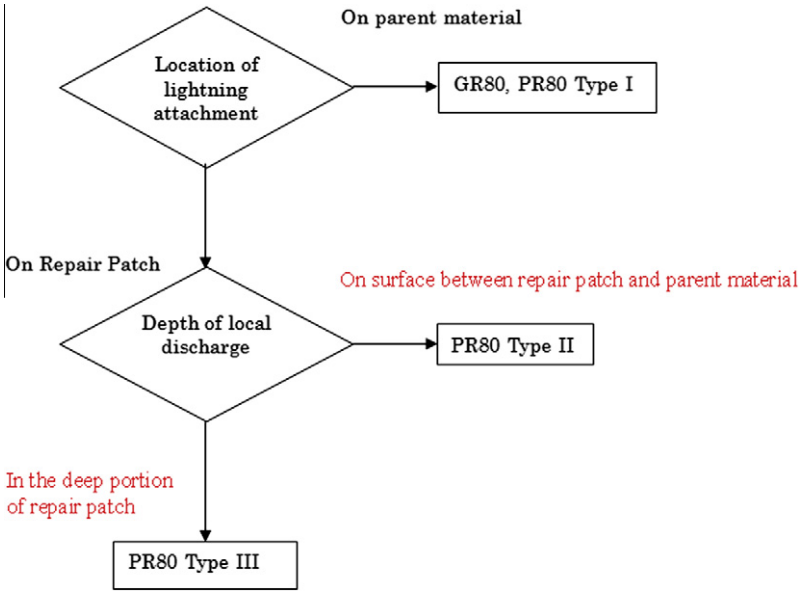

Fig. 26. Types of damage depending on specimen types and location and depth of lightning attachment point. (For interpretation of the references to color in this figure legend, the reader is referred to the web version of this article.)

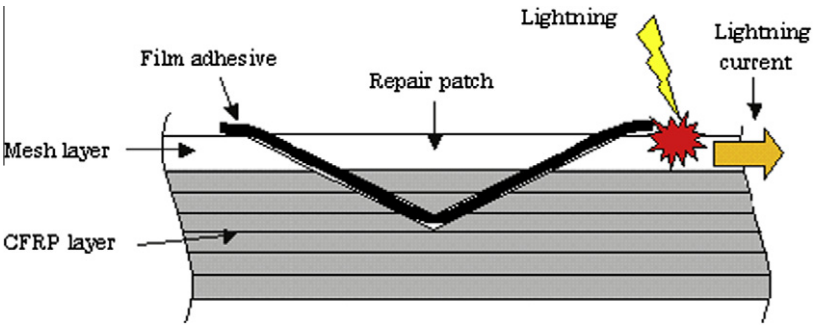

Fig. 27. Schematic of damage mechanism for strike on parent material (outside patch). (For interpretation of the references to color in this figure legend, the reader is referred to the web version of this article.)

4. Discussion

In this section, the three damage morphologies observed for poor repair specimens (PR80) are discussed qualitatively on the basis of visual inspections, C-scan results and destructive microscopy. The three categories of damage state, and associated residual strength reductions, are related to the location in the plane and through the thickness of the electrical discharge, as summarized in the diagram of Fig. 26. When lightning strikes a "poor" repair specimen, three possible scenarios can manifest. If the location of the strike falls outside of the repair patch (i.e. somewhere on the parent material, Fig. 27), the extent of the visible and internal damage is approximately identical to mesh-protected non-repair specimen (M80 and MP80), as well as a "good" repair specimen (GR80). The majority of the damage is confined to a protective copper mesh layer, while the majority of the carbon fiber remains intact. This is the scenario encountered for PR80 Type I specimens.

If the lightning attaches somewhere on the surface of the repair patch, the electric current flow can either remain on the surface and follow the copper mesh, or bury itself in the laminate under the mesh. These two different electrical flow paths are thought to be responsible for the different damage types observed. Fig. 28 shows the close-up picture of the specimen PR80 (Type II) taken with dark field contrasting technique to facilitate the detection of inter- and intra-laminar cracks. For this specimen there exist two sets of separate longitudinal cracks. It is likely that the two cracks are initiated by different sources at different depths. The one in proximity of the surface is the primary damage source of the specimen Type II. On the other hand, the one that originates deeper within the laminate is the main contributor to the damage on the specimen Type III. Both sets of cracks do exist in a single specimen simultaneously.

If the lightning attaches to the center of the scarf repair material, but remains on the surface, the electrical discharge is spread out over the entire area of the patch up to the point where it reaches the edge of the patch itself. The electrical current encounters the discontinuity around the circumference of the patch, at which point it leads to secondary electric discharges along with extensive heating, which causes fiber fracture and matrix vaporization, Fig. 29A–C. This is the scenario encountered for PR80 Type II specimens, which exhibit similar damage resistance and tolerance characteristics as unprotected specimens (N80 and P80). The concentration of the lightning current near the material surface is mainly due to the presence of the highly conductive copper mesh layer, the anisotropic electric properties of the carbon fiber layers, and the so-called "skin effect". The electric conductivity in the plane is more than 1000 times higher than the through-the-thickness conductivity, hence the current's favored path is along the plane rather than through the thickness. The skin effect refers to the phenomenon by which a current with high frequency of 101 kHz (the 10–90% rise-time of the simulated lightning is 3.5 μsec) flows in a very narrow skin on a conductor because of the interaction with the magnetic field. For instance, the skin depth of copper becomes 0.0079 in. (0.2 mm) under the above condition. The skin effect can interfere with the electric current in a through-the-thickness direction by limiting the effective cross-section of the copper mesh. As a result, the skin effect can facilitate the current concentration on the mesh layer. When this surface current flow reaches the edge of the patch it tries to create a bridge across the gap, between the patch and the parent material, in the form of local electric discharge through either surrounding air or dielectric epoxy. Most likely the local discharge takes place via air because of its lower breakdown voltage than epoxy layer. Pryzby and Plumer

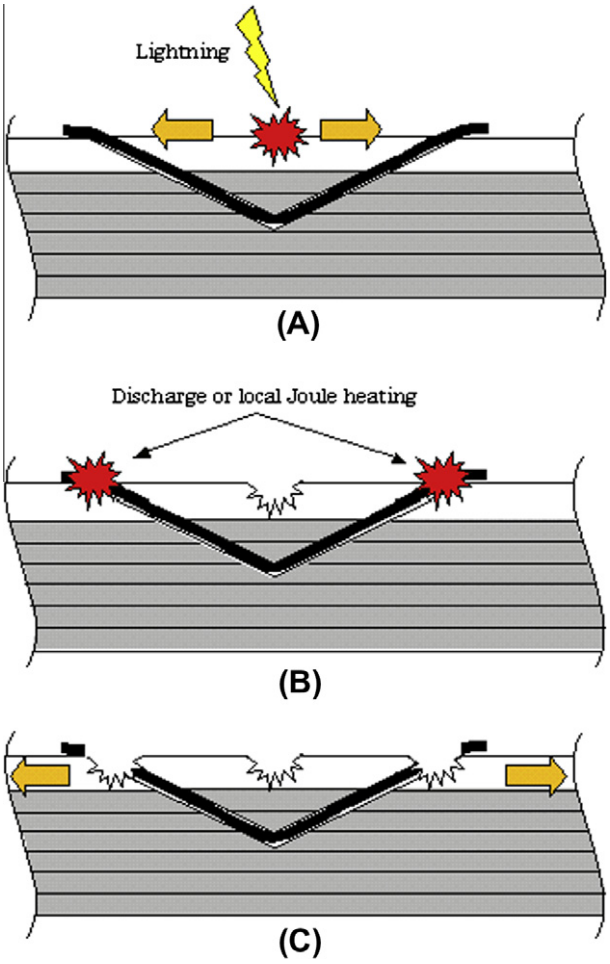

Fig. 29. (A–C) Schematic of damage mechanism for strike on repair patch near the surface. (For interpretation of the references to color in this figure legend, the reader is referred to the web version of this article.)

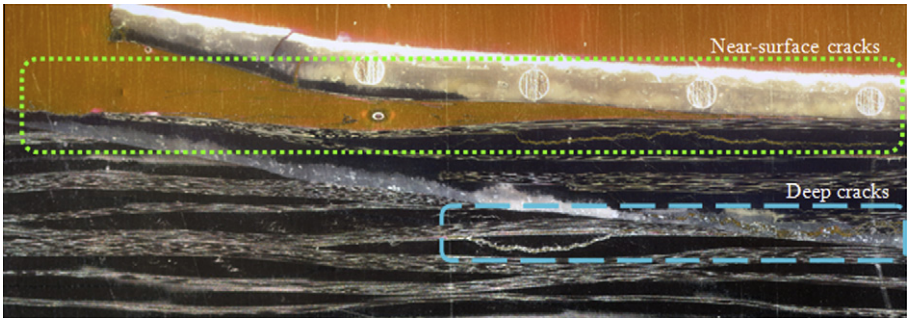

Fig. 28. Close-up microscopic picture of specimen PR80, Type II damage, using dark field contrasting technique. (For interpretation of the references to color in this figure legend, the reader is referred to the web version of this article.)

[23] studied the influence of lightning current injection without an electric arc on a single lap joint specimen, which was two CFRP adherends bonded together with a single layer of dielectric epoxy adhesive. Their results showed that a breakdown occurred at the edge of the specimens and, hence, an electric arc was not generated through the epoxy adhesive layer but through the surrounding air. They speculated that this was due to the lower breakdown voltage of air as compared to that of the adhesive layer. It is reasonable to assume that the same thing can happen to the poor repair specimen of our study for the following two reasons: the similarity of the specimen configuration of the dielectric epoxy between the repair patch and parent material, and the damage distribution which was concentrated on the near-surface of the gap between the patch and the parent material. Consequently, it is believed that the secondary local electric arc through the surrounding air between the edges of the repair patch and the parent material is formed all around the circumference of the repair patch, then high temperature and pressure emanating from the local arc cause damages on the neighboring adhesive epoxy layer, CFRP layers and protective copper mesh layers.

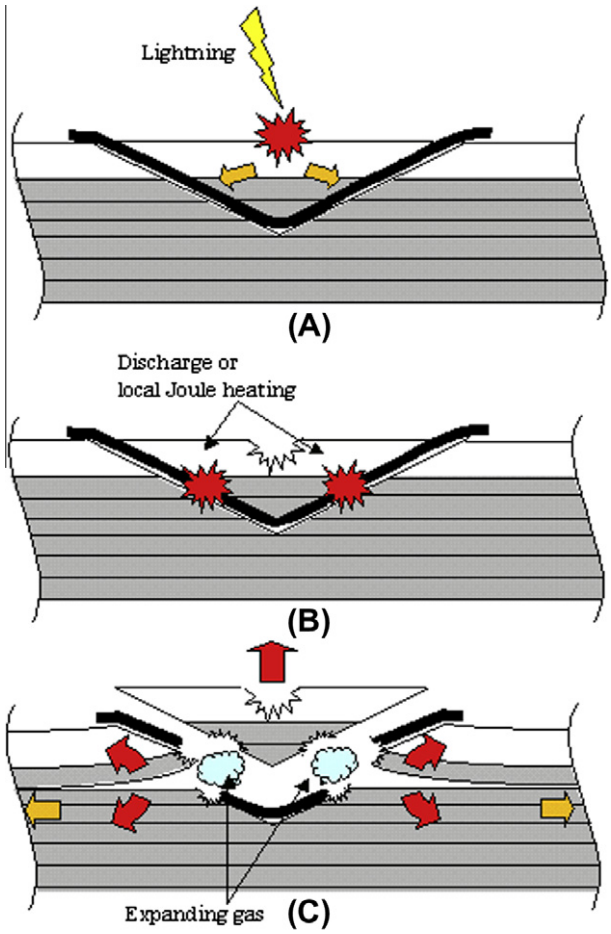

Fig. 30. (A–C) Schematic of damage mechanism for strike on repair patch in depth. (For interpretation of the references to color in this figure legend, the reader is referred to the web version of this article.)

Lastly, if the lightning attaches to the center of the scarf repair material, but penetrates through the thickness of the laminate because of excessive discontinuities along the surface path, the electrical discharge occurs within the depth of the laminate, Fig. 30A–C. If the dielectric strength of the gap between the patch and the parent material is enough high to prevent (or limit) electric arcing across the gap, the electric current inevitably spreads through the CFRP layers under the mesh to seek weak points of the specimen. Once the electric arc is successfully formed, the rapid Joule heating associated with fiber pyrolysis and resin vaporization leads to the expansion of the gases generated. The resulting overpressure pushes the repair patch outward and leads to complete disbonding of the patch from the parent laminate. Unlike the surface damage formation process which is open to the ambient air, the generated gases are confined to a small volume inside the specimen and, therefore, the effect of mechanical loading caused by the overpressure becomes devastating while the extent of thermal effects, such as melting and evaporation, is limited. In a sense, the energy released through this event is effectively used for initiating and expanding the damage of the material. This damage scenario is peculiar to PR80 Type III specimens. A comparison between the C-scan image and visual inspection of a PR80 Type III specimen, Fig. 31, shows that state of damage below the surface is much larger than the visible damage. This observation is the cause for the even greater area of damage observed in the case of PR80 Type III specimens compared to PR80 Type II specimens. Furthermore, the internal damage tends to be biased in the direction perpendicular to the electrical flow path (the longitudinal or 0°), while the outer damage is circular and the same size as the scarf repair patch. Lastly, multiple secondary electric discharges, individuated by distinct burn marks, can be seen at the periphery (around the circumference) of the scarf repair area.

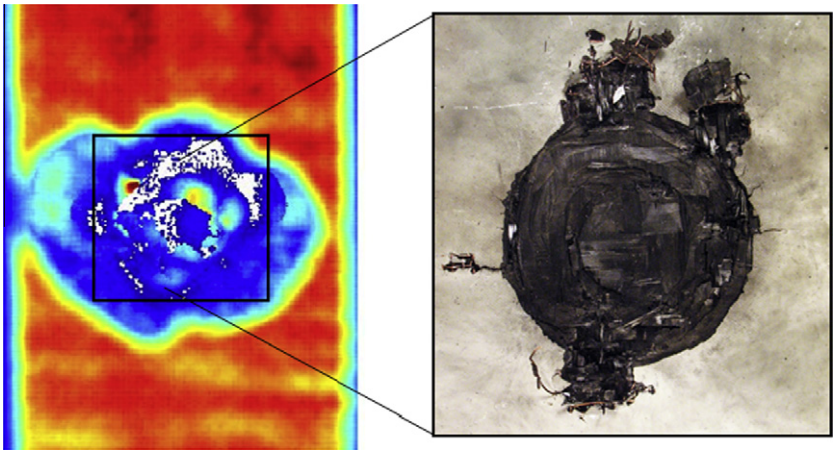

Fig. 31. Details of internal and external damage on PR80 Type III specimen, where the scarf patch is ejected during the lightning strike event and a much broader damage area can be observed below the surface. (For interpretation of the references to color in this figure legend, the reader is referred to the web version of this article.)

5. Conclusions

This experimental investigation was focused on understanding the implication of having a structural scarf repair on the outer skin of a composite structure with regards to lightning strike damage resistance and tolerance. Carbon fiber/epoxy composite specimens were manufactured using liquid resin infusion, incorporating a copper wire mesh for lightning strike protection on the outer surface. The cured specimens were subjected to scarf repair, which removes a portion of the wire mesh and half of the thickness of the carbon fiber substrate. Test results showed that the bonded scarf repair managed to re-establish the structural integrity of the laminate. However, the electrical integrity of the specimens is deliberately not re-established for all specimens. In the case of the so-called "good" repair, the repair copper mesh is overlapped on the parent mesh surrounding the repair area, thereby re-establishing the electrical path. For the so-called "poor" repair, the repair copper mesh is placed in a way to leave a small gap with the parent mesh, thereby preventing the electrical path to be fully reconstituted. The repaired specimens are then painted with aircraft-grade acrylic paint, and subjected to simulated lightning strike at the location of the repair. The damage state was evaluated both by ultrasonic C-scan imaging and through micrographic section. Among the variables tested, the copper mesh protection has the largest influence in reducing the overall damage area, by preventing the electrical discharge from damaging the underlying carbon fiber plies. Specimens tested without the copper wire mesh exhibited large damage area and significant residual strength reduction. The outer paint layer, which is a dielectric, has the effect of increasing slightly the damage depth as well as decreasing the damage area as compared to the unpainted specimens. For the specimens containing a scarf repair it was shown that a "good" repair behaves structurally and electrically in the same fashion as a protected pristine specimen, and thus exhibits negligible surface damage and residual strength reduction. For the case of "poor" repair, three different scenarios may manifest, depending on the location of the lightning attachment point with respect to the repair area. If the lightning strikes away from the repair area, there is no difference in damage area and residual strength between a poor repair and a good repair or a pristine specimen. If the lightning strikes onto the patch, the resulting damage area and residual strength reduction are at the very least as catastrophic as an unprotected specimen, and in cases much more devastating, causing the entire scarf patch to disbond during the lightning strike. Therefore, if an aircraft panel is somehow damaged and undergoes a scarf bonded repair, it is imperative that its electrical as well as structural integrity be reconstituted. To re-establish the electrical path between repair and parent materials, it is necessary to overlap the copper mesh on both sides. Failure to do so may lead to catastrophic results, as a poor repair specimen behaves at least the same, and at times worse, than a specimen without copper wire mesh.

Acknowledgments

The authors would like to acknowledge the fundamental contributions of their colleagues Art Blair, Robert Gordon, Prof. Tom Mattick, Prof. Uri Shumlak and undergraduates Andy Le, Danny Le, and Natalie Larson. They would also like to thank Robert Steinle, Diane Heidlebaugh, and Art Day (The Boeing Co.) for their technical support and expert advice. Mr. Akira Yokoyama of the Japanese Ministry of Defence is also gratefully acknowledged for sponsoring Mr. Kawakami's doctoral research.

References

[1] Nagao Y. Low cost composite manufacturing technology development program for wing structure by JAXA. In: Keynote lecture, 14th US–Japan conference on composite materials. Dayton, OH; September 2010.
[2] Sugimoto S, Aoki Y, Hirano Y, Nagao Y. A study on non-destructive evaluation of VaRTM composite structure. In: 13th US–Japan conference on composite materials. Tokyo, Japan; June 2008.
[3] Koiwai H. Composite application for Japan's new regional jet aircraft by mitsubishi aircraft. In: Keynote lecture, 13th US–Japan conference on composite materials. Tokyo, Japan; June 2008.
[4] Miller A. The Boeing 787 Dreamliner. In: Keynote address, 22nd American society for composites technical conference. Seattle, WA; September 2007.
[5] Reggiani M, Feraboli P. Carbon fiber composites: the key technology for the 21st century. Keynote lecture, ASME IMECE, Orlando, FL; November 2009.
[6] Feraboli P, Deleo F, Wade B, Rassaian M, Higgins M, Byar A, et al. Predictive modeling of an energy-absorbing sandwich structural concept using the building block approach. Composites (Part A) 2010;41(6):774–86.
[7] Rupke E. Lightning direct effects handbook. Lightning Technologies Inc. Report no. AGATE-WP3.1-031027-043-Design guideline; March 1, 2002.
[8] Fisher FA, Plumer JA. Aircraft lightning protection handbook. DOT/FAA/CT-89/22; September 1989.
[9] Welch JM. Repair design, test, and process considerations for lightning strikes. In: 3rd FAA/EASA/Boeing/Airbus joint workshop on safety and certification. Amsterdam, NL; May 2007.
[10] Yamanaka J. Japan Airlines perspective on application and field experiences for composite structures. In: 4th FAA/EASA/Boeing/Airbus joint workshop on safety and certification. Tokyo, JP; June 2009.
[11] Nakayama N. Field experience: lightning strike damage of ANA B767. 4th FAA/EASA/Boeing/Airbus joint workshop on safety and certification. Tokyo, JP; June 2009.
[12] Heidlebaugh D, Avery W, Uhrich S. Effect of lightning currents on structural performance of composite materials. In: International conference on lightning and static electricity, SAE paper no. 2001-01-2885, Seattle, WA; September 2001.
[13] Feraboli P, Miller M. Damage resistance and tolerance of carbon/epoxy composite coupons subjected to simulated lightning strike. Composites (Part A) 2009;40(6–7):954–67.
[14] Feraboli P, Kawakami H. Damage of carbon/epoxy composite plates subjected to mechanical impact and simulated lightning strike. J Aircraft 2010;47(3):999–1012.
[15] Fawcett A, Oakes G. Boeing composite airframe damage tolerance and service experience. 2nd FAA/EASA/Boeing/Airbus joint workshop on safety and certification. Chicago, IL; July 2006.
[16] Chesmar E. United Airlines perspectives on composite maintenance challenges and regulatory issues. 4th FAA/EASA/Boeing/Airbus joint workshop on safety and certification. Tokyo, JP; June 2009.
[17] Damage Resistance, Durability, and Damage Tolerance, MIL-HDBK-17, vol. 3, Rev. F. West Conshohocken (PA): ASTM International; 2002 [chapter 7].
[18] Supportability, MIL-HDBK-17, vol. 3, Rev. F. West Conshohocken (PA): ASTM International; 2002 [chapter 8].
[19] Ahn S, Springer G. Repair of composite laminates, FAA technical report DOT/FAA/AR-00/46; December 2000.
[20] Tomblin JS, Salah L, Welch JM, Borgman MD. Bonded repair of aircraft composite sandwich structures. FAA technical report DOT/FAA/AR-03/74; February 2004.
[21] Aerospace recommended practice ARP 5412. Aircraft lightning environment and related test waveforms, SAE; 1999.
[22] ASTM C393, standard test method for flexural properties of sandwich constructions, vol. 15.03. West Conshohocken (PA, USA): ASTM International; 2009.
[23] Pryzby JE, Plumer JA. Lightning protection guidelines and test data for adhesively bonded aircraft structures. NASA contractor report 3762; 1984.